Filtering the surface EMG signal: Movement artifact and baseline noise contamination

Carlo J. De Luca [a,b], L. Donald Gilmore [b], Mikhail Kuznetsov [b], Serge H. Roy [b,*]

[a] Delsys Inc., Boston MA, USA
[b] NeuroMuscular Research Center, Boston University, 19 Deerfield St, Boston MA, USA

ARTICLE INFO

ABSTRACT

The surface electromyographic (sEMG) signal that originates in the muscle is inevitably contaminated by various noise signals or artifacts that originate at the skin-electrode interface, in the electronics that amplifies the signals, and in external sources. Modern technology is substantially immune to some of these noises, but not to the baseline noise and the movement artifact noise. These noise sources have frequency spectra that contaminate the low-frequency part of the sEMG frequency spectrum. There are many factors which must be taken into consideration when determining the appropriate filter specifications to remove these artifacts; they include the muscle tested and type of contraction, the sensor configuration, and specific noise source. The band-pass determination is always a compromise between (a) reducing noise and artifact contamination, and (b) preserving the desired information from the sEMG signal. This study was designed to investigate the effects of mechanical perturbations and noise that are typically encountered during sEMG recordings in clinical and related applications. The analysis established the relationship between the attenuation rates of the movement artifact and the sEMG signal as a function of the filter band pass. When this relationship is combined with other considerations related to the informational content of the signal, the signal distortion of filters, and the kinds of artifacts evaluated in this study, a Butterworth filter with a corner frequency of 20 Hz and a slope of 12 dB/oct is recommended for general use. The results of this study are relevant to biomechanical and clinical applications where the measurements of body dynamics and kinematics may include artifact sources.

© 2010 Elsevier Ltd. All rights reserved.

1. Introduction

The surface electromyographic (sEMG) signal contains the signal that originates in the muscle and various noise components which are endemic and unavoidable. These noise components contaminate the sEMG signal and may lead to an erroneous interpretation of the signal. This is especially the case when the signal is obtained during dynamic contractions and when it is meant to provide information concerning the physiology and anatomy of muscles.

Beyond using effective methods of locating and securing the sEMG sensor to the skin (De Luca, 1997; Roy et al., 2007), one of the simplest and most direct means of increasing the fidelity of the sEMG signal is to filter the maximum amount of noise while retaining as much of the desired EMG signal frequency spectrum as possible. The frequency spectrum of the sEMG signal collected with commonly used sensors ranges from 0 to 400 Hz, depending on the electrode spacing, the amount of fatty tissue between the skin and the muscle tissue, the shapes of the action potentials, and

muscle type (Basmajian and De Luca, 1985). The bandwidth is generally greater if the sensor is placed over the insertion of the muscle fibers into the tendons or on top of the innervation zone of the muscle. However, such a placement is not advisable because the amplitude of the signal is sensitive to this precise location (Beck et al., 2008). At the high-frequency end of the sEMG signal spectrum, the low-pass filter corner frequency (the boundary of the filter's frequency response where signal energy is attenuated by 3 dB), should be set where the amplitude of the noise components surpasses that of the sEMG signal. Consequently, it is preferable for the high end of the sEMG frequency spectrum to have a low-pass corner frequency in the range of 400–450 Hz.

At the low-frequency end of the spectrum, the choice of the location of the high-pass filter corner frequency is more involved because several noise sources contribute signals whose low-frequency spectra overlap with that of the sEMG signal. Consequently, the determination of the filter characteristics in this region has been a focus of attention. Over the past three decades, various recommendations and standards have been put forth; they are: (a) the recommendations of the International Society of Electrophysiology and Kinesiology (Winter et al., 1980) which recommended a high-pass corner frequency of 20 Hz; (b) Standards for Reporting EMG Data (Merletti, 1999) which

---

* Corresponding author. Tel.: +1 617 358 0718; fax: +1 617 353 5737.
 E-mail address: sroy@bu.edu (S.H. Roy).

recommended 5 Hz; (c) the requirements of the Journal of Electromyography and Kinesiology which requires a corner frequency of 10 Hz for a report to be published; and (d) the Surface EMG for Noninvasive Assessment of Muscles (SENIAM) recommendations (Stegeman and Hermens, 1998) which recommends 10–20 Hz.

The SENIAM recommendation is based on a survey of the practices of various laboratories identified via the sEMG literature, rather than data from empirical studies. Hence, that report only reflects the convention of a self-selected group of EMG practitioners. The only available empirical data has been provided by van Boxtel et al. (1998) and van Boxtel (2001) who recommend a high-pass corner frequency range of 15–28 Hz when detecting signals from facial muscles, including blinking eye lids. There are no empirically based specifications for filtering sEMG data from limb muscles.

There are several intrinsic and extrinsic sources of low-frequency noise that may contaminate the sEMG signal. The two extrinsic noise sources, the *power line noise* and the *cable motion artifact*, can be almost totally eliminated with modern electronics technology and appropriate circuit design. The two intrinsic noise sources originate in the electronics of the amplification system (*thermal noise*) and at the skin-electrode interface (*electrochemical noise*), respectively (Huigen et al., 2002). Together, these noise sources form the *baseline noise* which is detected whenever a sensor is attached to the skin. An additional noise source, the *movement artifact noise*, also originates at the electrode-skin interface. It is generated when: (a) the muscle moves underneath the skin, and (b) when a force impulse travels through the muscle and skin underlying the sensor causing a movement at the electrode-skin interface. The resulting time-varying voltage produced across the two electrodes can be the most troublesome of noise sources and requires the most attention.

In this report we provide empirical evidence to ascertain a reasonable value for the corner frequency for removing the low-frequency noise components; especially those generated by the movement artifact. Removal of these components renders the sEMG signal more useful for practical applications. Our approach selected different high-pass corner frequencies typically used to filter the sEMG signal, and compared their performance under controlled noise conditions.

2. Methods

The methods were designed to elicit a large number (>300) of controlled isometric contractions with and without movement artifact. Seven healthy male subjects and five healthy female subjects (mean age 30.3; range 19–63 years) volunteered for the study after providing institutionally approved written informed consent. Two muscles, the tibialis anterior (TA) and the first dorsal interosseous (FDI), were chosen for this study because of their differences in size and skin thickness, which influence the sEMG signal spectra of the two muscles (Basmajian and De Luca, 1985) and thereby provide diverse signal sources for the investigation.

The sEMG signals were detected with DE-2.1 sensors (Delsys Inc.) and were amplified by a Bagnoli™ 8-channel system (Delsys Inc.) with a modified band pass of 0.15 Hz (6 dB/oct) to 450 Hz (24 dB/oct). The skin was cleaned by mildly scrubbing it with 70% isopropyl alcohol. The sensors were attached to the skin with a double-sided adhesive interface tailored to match the contours of the sensor. The sEMG sensor was located on the belly of the muscle at a position distant from the innervation zones and the muscle tendon interface, following the recommendations of De Luca, 1997 and Saitou et al., 2000. A Dermatrode® HE-R (American Imex) electrode (5.08 cm dia.) was located on the back of the left hand to provide a reference.

In order to monitor the movement artifact, accelerometers were attached in the proximity of the sEMG sensors (dynamic range ±5 g; maximum resolution 2 mg; bandwidth >250 Hz); refer to Fig. 1. For the FDI, the accelerometer (Motorola MMA1220D) was placed on top of the sEMG sensor to register normal acceleration, as would likely be produced when movement artifacts caused by direct contact with the sensor occur. For the TA, the accelerometer (Analog Devices ADXL105JQCL) was placed distal to the sEMG sensor to register shear force, as
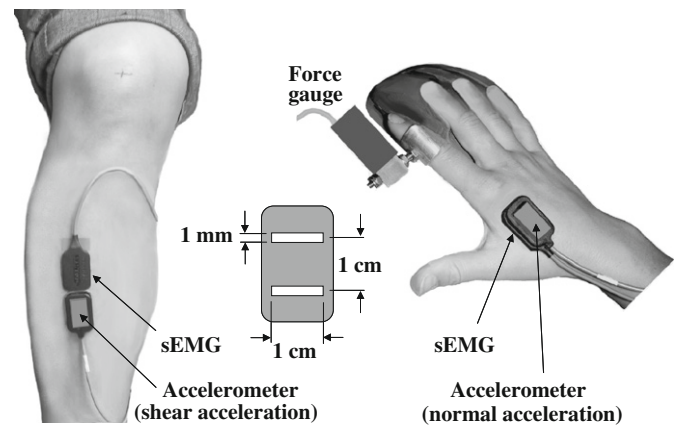
Fig. 1. Image of the experimental data collection. The sensor locations are shown for the Tibialis Anterior (TA) muscle (left) and First Dorsal Interosseous (FDI) muscle (right). The sEMG sensors contain two electrodes consisting of parallel bars spaced 1 cm apart. A uni-axial accelerometer was placed below the EMG sensor on the TA muscle to measure shear acceleration and another above the FDI muscle to measure normal acceleration.

would occur for example by impacts to the limb while walking. The raw data from the sEMG and accelerometer sensors were sampled at a rate of 5 KHz and stored in digital format using EMGworks® Acquisition software.

Data were acquired while the subjects were seated with their hand and lower limb secured into an apparatus that constrained the muscles to isometric contractions (Adam and De Luca, 2005). The protocol for producing artifacts was designed to replicate two conditions; one in which perturbations are externally applied directly to the sensor and the second in which perturbations to the sensor are produced as a result of body movement. While there are numerous methods to apply mechanical disturbances to the sensor, we selected more forceful perturbations which include those that might be encountered in work and sports environments. For the case of externally applied perturbations, movement artifact producing force was applied by tapping the sensor placed on the FDI muscle. We purposefully tapped directly on the sensor to maximize the effect of the mechanical disturbance. The acceleration profile was monitored and used to guide the experimenter in applying similar taps to the sensor. For the second condition, we produced a perturbation to the body that would be similar to that which occurs during the heel strike phase of gait. The sensor located on the TA muscle of the leg was indirectly perturbed by striking the supra-patella region of the flexed knee with the open palm of the hand, simulating heel strike during gait. With practice, we were able to apply a force on the knee in a manner that produced accelerations to the sensor that were similar to those obtained in a pilot study where heel strike was accentuated by having the subjects walk without shoes. This simulation provided a controlled means of obtaining the data at various isometric contraction levels.

The experimental protocol began with the acquisition of the maximum voluntary contraction (MVC) level by asking the subject to contract as strongly as possible and to hold the contraction for 3 s. This procedure was repeated two more times with rest intervals of 3 min. The highest peak value of the three contractions was chosen as the MVC level. After a rest period of 3 min, the subjects were asked to perform three constant-force isometric contractions at 0%, 10%, and 50% MVC level, with a rest period of 3 min between each contraction. Each contraction was sustained for 20 s. The 0% MVC was executed with the muscle completely relaxed as evidenced by no discernable sEMG signal. This datum sample was used to obtain the baseline noise of the system. Three additional 0% MVC level contractions were performed, each with a sequence of 20 artifact-inducing taps applied at 2 s intervals.

3. Results

The data were filtered at the three representative high-pass corner frequencies (10, 20, 30 Hz) and normalized to the same data high-pass filtered at 1 Hz. The three corner frequencies were processed using two different filter slopes at 12 and 24 dB/oct to initially determine the affect of the filter slope on the signal spectrum. The influence on the spectral shapes was minor (less than 1% difference in RMS), and consequently, we report the results from only one filter slope. The 12 dB/oct Butterworth filter slope was selected because it exhibited less overshoot and has a faster settling time in response to signal transients.

Fig. 2 presents samples of movement artifact detected by the sEMG and accelerometer sensors for the FDI and the TA muscle in two subjects recorded at full bandwidth (1–450 Hz). The data confirm that the sequence of perturbations produced similar, but not identical, acceleration profiles, as intended. Fig. 2 demonstrates that the acceleration profiles of the FDI are similar in amplitude for both subjects. Despite this consistency, the resultant sEMG movement artifacts were highly variable; both within the same experiment on a given subject as well as between subjects when comparing data from the same muscle. These variations are expected because of the flexibility of the skin and the sensitivity of the electro-chemical interface between the electrode contact and the skin.

An inspection of the sEMG spectrum for the signal in Fig. 3 (Panel B) reveals that most of the power is contained between 20 and 200 Hz. The movement artifact signal in Panel C, recorded under quiescent conditions, exhibits its greatest spectral components at the lower frequencies, dropping off rapidly beyond 20 Hz. A similar behavior of the spectrum is displayed by the signal in Panel D which also contains the sEMG signal. These spectral plots indicate that a corner frequency of 10 Hz may not remove sufficient noise spectral components.

Two examples of the effects of corner frequency on the sEMG signal are shown for different muscles in the same subject (Fig. 4), where the profiles of the movement artifacts are dissimilar and they corrupt the sEMG signal in noticeably different ways. The artifacts ranged from near baseline noise levels to extreme

instances where the artifact component of the signal exceeded the EMG component by over 3X the signal level during a 50% MVC contraction. As the corner frequency is increased, the artifact component is reduced in both muscles and is visually absent in the sEMG signal plots of the TA filtered at 10 Hz. However, the spectral plots reveal that the movement artifact component continues to influence the shape of the sEMG signal spectra until approximately 20 Hz. The spectral plots indicate that the 10 Hz filter does not fully remove the artifact; and the 30 Hz filter, while successfully attenuating the artifact, also removes a portion of the lower frequency components of the sEMG signal. The effect of the signal loss using the 30 Hz corner frequency is even more pronounced in the TA muscle which has proportionally more energy distributed in the lower frequency range compared to the corresponding energy distribution of the FDI muscle.

The signal loss is more clearly seen in Fig. 5, which presents the mean ($\pm$ SD) values of the RMS signal loss for each of the sEMG signal and noise components as a function of the corner frequencies for all the subjects. The RMS amplitude of the sEMG signal (at 10% and 50% MVC) decreases as the corner frequency increases. In the FDI muscle, the total decrease in amplitude for both contraction levels ranges from approximately 3–4%. In the TA muscle the total decrease for both contractions ranges from approximately 4–7%. The baseline noise (middle trace) decreases sharply by approximately 40% at 10 Hz, 47% at 20 Hz, and 51% at 30 Hz for both muscles. The baseline noise and movement artifact (lower trace) presents a more substantial decrease ranging from
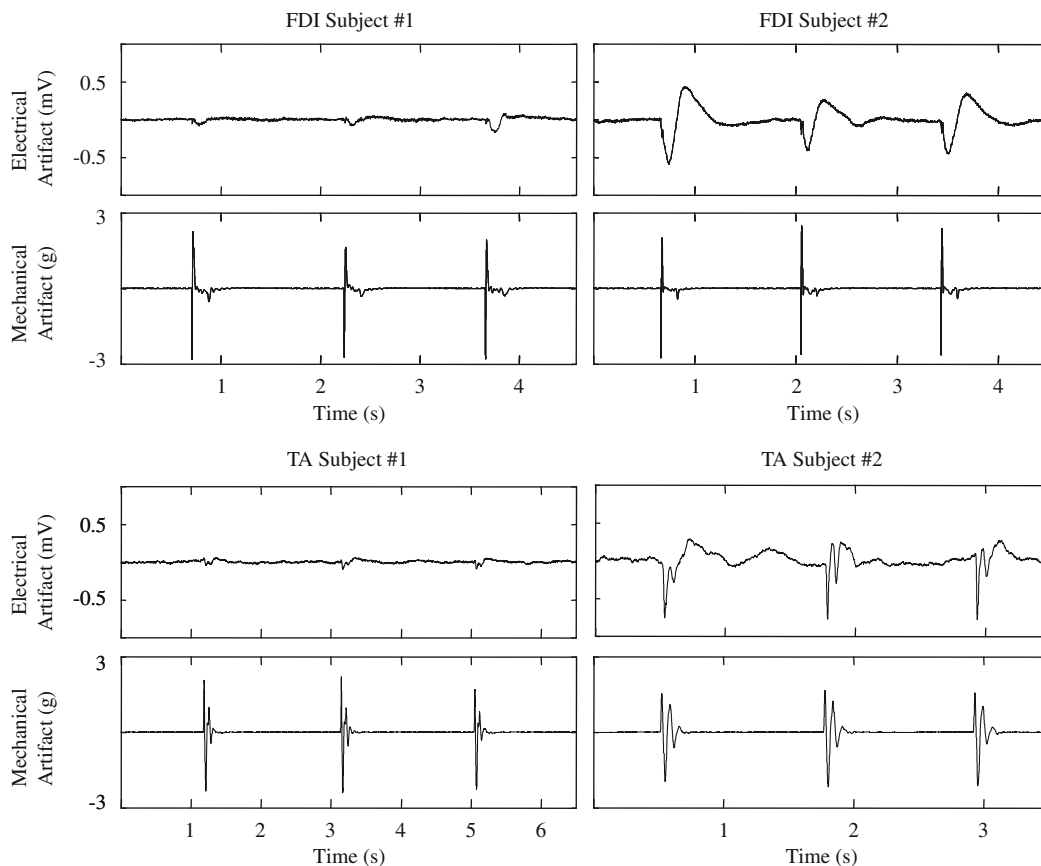
Fig. 2. Samples of the movement artifact detected by the sEMG sensor and the accelerometer sensor. Data are from Subject #1 (left) and Subject #2 (right) for both the First Dorsal Interosseous (FDI) and the Tibialis Anterior (TA) muscles. The movement artifact, recorded during the 0% MVC test condition, were filtered with a 2-pole Butterworth filter with a high-pass corner frequency at 1 Hz (12 db/oct) to allow for the full spectral content. The plots are set to the same amplitude scale to facilitate comparison across samples. Note that the acceleration profiles of the FDI are similar in amplitude for both subjects. Despite this consistency, the resultant sEMG movement artifacts were highly variable; both within the same experiment on a given subject as well as between subjects when comparing data from the same muscle. The data from the TA muscle show similar variability, but to a lesser degree. [Note that the movement artifact signals also contain the baseline noise signal. However, the amplitude of the baseline noise is several orders of magnitude smaller and is barely perceivable in the plots].
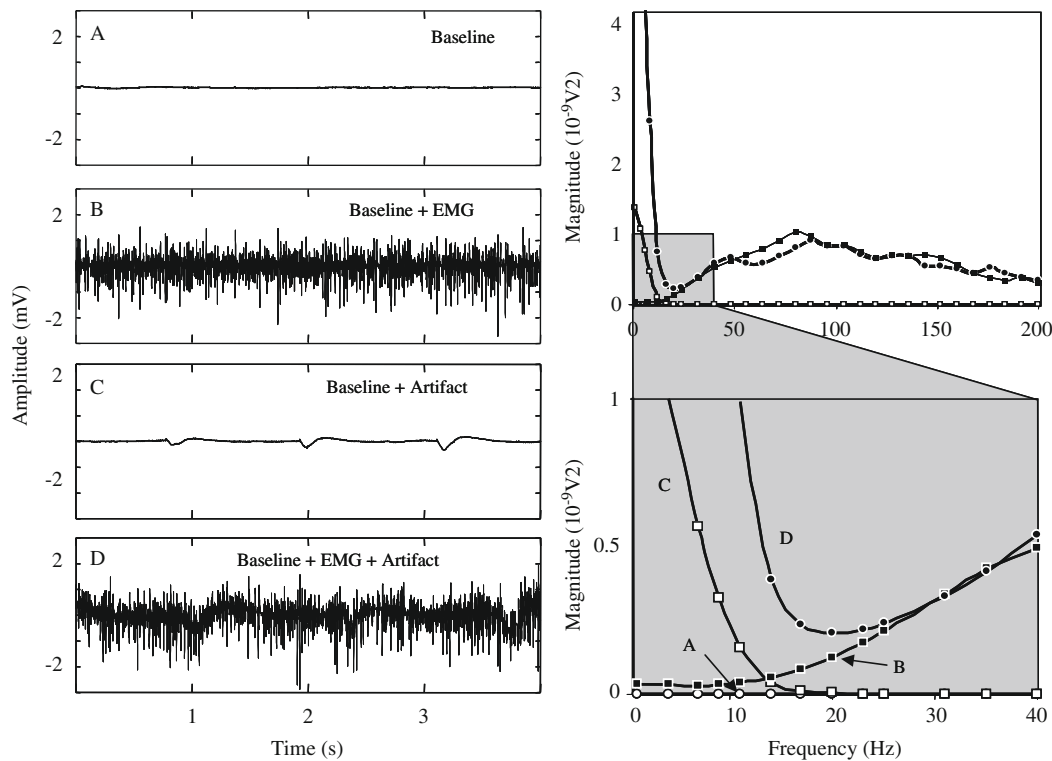
Fig. 3. The time domain and spectral characteristics of the baseline noise, the sEMG signals, the induced movement artifact signals, and the sEMG signals contaminated by movement artifacts. Panel A presents the baseline noise obtained during a 0% MVC; Panel B presents the sEMG signals obtained during a 50% MVC; Panel C presents the movement artifact signal during quiescent baseline conditions; and Panel D represents the sEMG signal and the movement artifact signal during a 50% MVC. In all cases the signals contain the baseline noise consisting of the electrical noise from the preamplifier and the skin-electrode interface. The signals were high-pass filtered at a 1 Hz corner frequency (12 dB/oct) to preserve the spectral content of the signal. The spectra of the individual signals are shown on the right, with the lower traces showing the expanded low-frequency portion. All the plots are presented on the same amplitude scale to facilitate direct visual comparison.

69% to 83% at 30 Hz for both muscles. Post-hoc pair-wise statistical comparisons between the mean values in Fig. 5 were all significant at $p < 0.01$.

4. Discussion

The choice of using state of the art equipment minimized the influence of two extrinsic noise sources, the power line noise and the cable motion artifact, and one intrinsic thermal noise source originating in the electronics of the amplification system. This allowed us to focus on the noise components attributable to the electro-chemical noise at the skin-electrode interface and mechanical disturbance.

The sensors in this study had a fixed inter-electrode spacing of 1.0 cm. Sensors with electrodes spaced further apart detect sEMG signals having a more compressed frequency spectrum (Lindstrom et al., 1970). Because this study investigates the effect of filtering on the low-frequency part of the sEMG spectrum, the results also apply to sEMG signals detected with sensors having wider electrode spacing. The results of this study were derived from a protocol which attempted to reproduce artifact sources that may be problematic when utilizing sEMG analysis for evaluating gait and movement disorders (Pullman et al., 2000).

The selected experimental protocol for this study provided a data set from 12 subjects where the sEMG signal was contaminated by artifacts that exhibited a broad range of magnitudes from mild to severe levels for two different muscles. These variations in magnitude occur because of the flexibility of the skin and the sensitivity of the electro-chemical interface to mechanical perturbations. This range provided a comprehensive data set for

evaluating the effect of filtering on the reduction of the artifact component of the sEMG signal.

The results from the protocol were used to establish a relationship between different sEMG filter settings and signal quality. The data presented in Fig. 5, for instance, indicated that as the high-pass corner frequency was increased, the sEMG, noise, and movement artifact signals decreased. The effect of the corner frequency, however, was much greater on the noise and movement artifact signals than it was on the sEMG signal. The sEMG signals exhibited a relatively linear decrease in amplitude as a function of corner frequency, whereas the baseline noise and the movement artifact signals exhibited a non-linear decrease with increasing corner frequency. For these signals a substantial decrease occurred at 10 Hz and the decrease continued at a lower rate for the 20 and 30 Hz corner frequencies. Therefore, in a sEMG system designed for general use, it is wise to include a high-pass filter that reduces baseline noise and suppresses the movement artifact while minimizing the removal of the sEMG signal frequency content of the low-frequency components that would contain relevant information concerning the performance of the muscle. As shown in the spectral plots of Fig. 3, the sEMG signal spectrum increases in amplitude (trace B) with increasing frequency. In contrast, the spectrum of the movement artifact signal (trace C) decreases rapidly as a function of frequency. The corner frequency selection cannot be based solely on the sEMG signal-to-artifact ratio. While the signal-to-artifact ratio will continue to increase with higher corner frequencies, the rate of sEMG signal loss will also increase.

The optimal corner frequency for filtering sEMG signals contaminated with movement artifact may be determined by considering the percentage of movement artifact and the percentage of EMG signal loss as a function of frequency
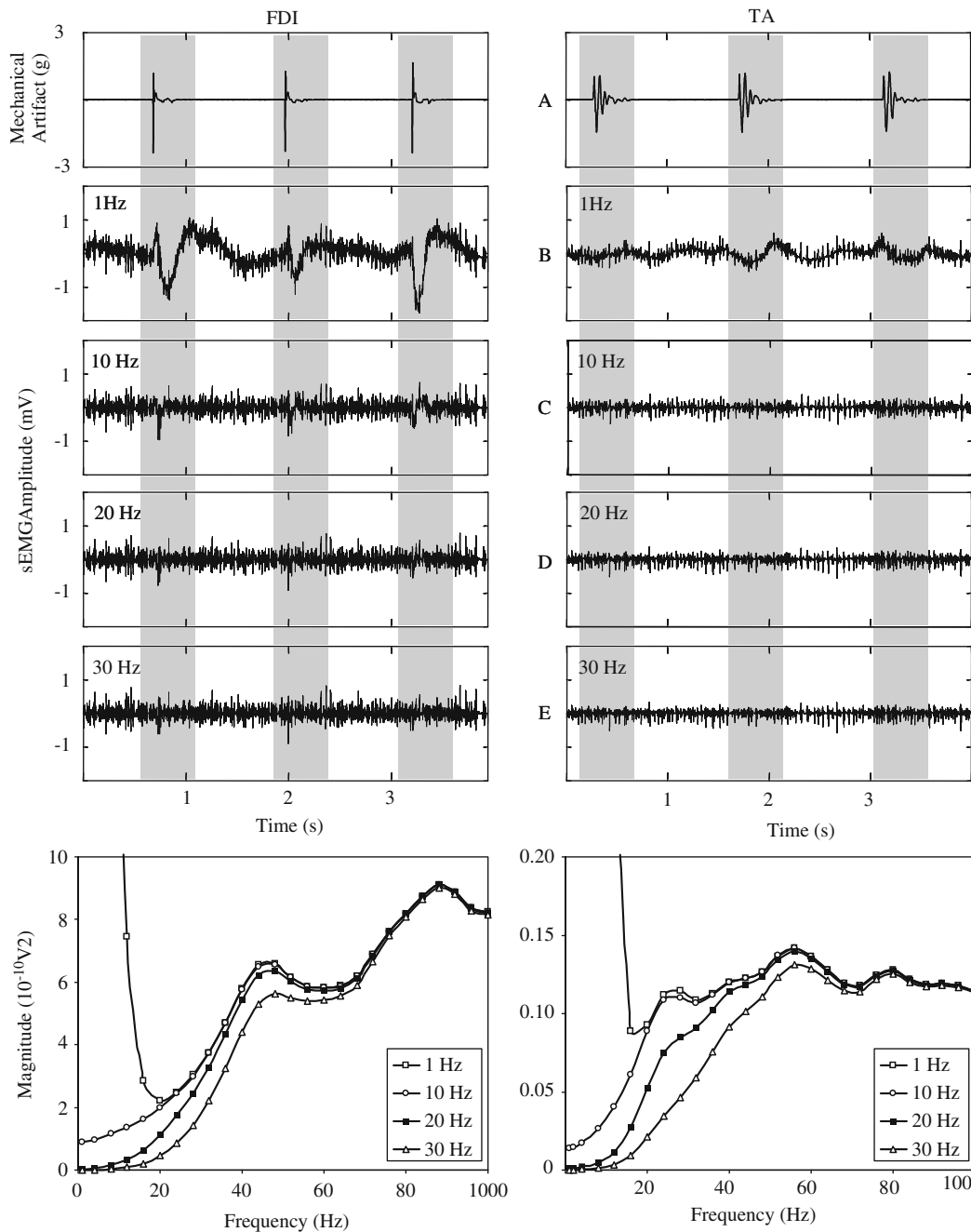
Fig. 4. Examples of artifact-contaminated sEMG signal filtered at different corner frequencies. The traces from the First Dorsal Interosseous (FDI) muscle on the left, and those from the Tibialis Anterior (TA) muscle on the right are from the same subject. FDI data were acquired during a 50% MVC and TA data were acquired at 10% MVC. Acceleration data for each muscle are presented in panel A. sEMG data are presented in panels B through E; these include baseline noise plus movement artifact. All are filtered at high-pass corner frequencies of 1, 10, 20, and 30 Hz, respectively, with a slope of 12 dB/oct. Note the shaded area which indicates the time location of the induced movement artifact. The corresponding frequency spectra are shown in the lower plots. Note the increased loss of the low frequency components of the 30 Hz high-pass filter spectrum, resulting in additional distortion of the sEMG signal.

increment. An example for the FDI muscle is plotted in Fig. 6. For the mechanical disturbances used in this study, the rate of artifact attenuation is greatest between 1 and 10 Hz increments, and it continues to decrease at lesser degrees between subsequent increments. Ultimately, the percent of loss in the movement artifact and the sEMG signals are equal when the corner frequency is incremented from 30 to 40 Hz. Further increases in corner frequency yield lower rates of improvement in movement artifact reduction, while incurring increasing sEMG signal losses.

While 30–40 Hz range may be an optimal compromise between artifact reduction and sEMG signal amplitude loss in

the FDI muscle, it comes at the expense of distorting the lower frequency components of the spectrum as can be seen in the 30 Hz trace of the FDI spectrum plot shown in the lower left panel of Fig. 4. The case is even more dramatic when the 30–40 Hz corner frequency range is applied to the TA muscle. For a 10% MVC contraction level of the TA muscle, the 30 Hz and 40 Hz corner frequencies cause a 7.4% and 13% loss in sEMG signal amplitude, respectively. These amplitude losses would be especially problematic for low level contractions which have lower signal-to-noise ratios where the loss would substantially degrade signal quality. Additionally, this amplitude loss is accompanied by a large
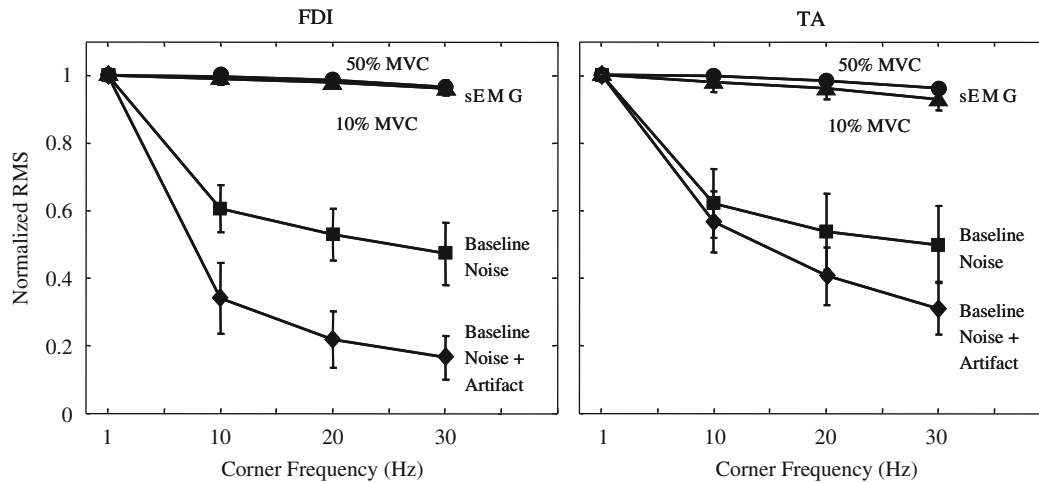
Fig. 5. Decreases in the RMS signal amplitude as a function of corner frequency is shown for the First Dorsal Interosseous (FDI) muscle (left), and the Tibialis Anterior (TA) muscle (right) from all subjects. The top two traces of the sEMG+baseline noise signals were obtained from contractions performed at 50% and 10% MVC, respectively. The bottom two traces are of the baseline noise, and the baseline noise plus the movement artifact signals detected, respectively. The RMS amplitude is normalized with respect to the value from the 1 Hz high-pass corner frequency filter. The symbols represent the mean value and the bars the standard deviation.
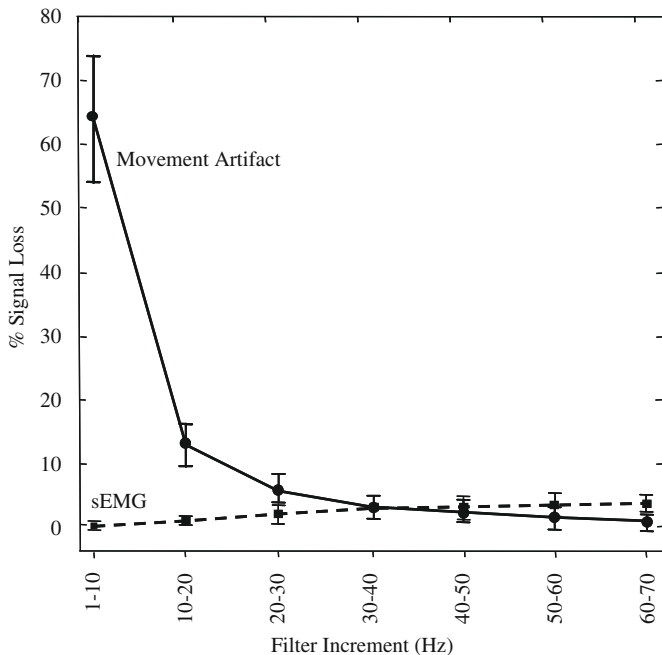
Fig. 6. Changes in the % signal loss for increasing high-pass filter increments are shown for movement artifact (solid line) and sEMG signal amplitude (dashed line). The symbols represent the mean value and the bars the standard deviation for data acquired from the FDI muscle in all subjects.

distortion in the low-frequency components of the spectrum as illustrated in the 30 Hz trace of the TA spectrum plot shown in the lower right panel of Fig. 4.

The choice of selecting the high-pass filter corner frequency is application and muscle dependant. For applications involving isometric contractions or natural and common movements, such as non-spastic gait measurements, the recommended corner frequency is 20 Hz. For those applications involving more vigorous movements than those applied in this study, such as during sports activities or in clinical situations involving patients with movement disorders, the corner frequency should be increased above 20 Hz by utilizing additional filtering to augment artifact suppression at the expense of additional sEMG signal

attenuation and spectral distortion. When considering muscle groups which have lower frequency distribution than those tested in this study, such as the lumbar paraspinal and quadriceps muscles (Roy et al., 1989; Gamet et al., 1993), a 20 Hz corner frequency is still appropriate.

Selecting a corner frequency below 20 Hz is not recommended. As may be seen in the spectral plots in Fig. 3, there is only a minor amount of energy below 20 Hz. Also, the energy between 10 and 20 Hz contains peaks whose amplitude corresponds to the average value of the firing rates of motor units and a width that is dependant on the standard deviation of the firing rate. See LeFever and De Luca (1976) and Basmajian and De Luca (1985) for details. The peak fluctuates especially during lower force contractions where the firing rate of motor units is more sensitive to the net excitation in the motoneuron pool. Consequently the energy in the sEMG signal below 20 Hz is unstable and does not provide a reliable contribution to the sEMG signal.

When limited to selecting a single high-pass corner frequency for general use, 20 Hz offers the best compromise for optimizing the desired informational content of the sEMG signal. This recommendation is consistent with the results of van Boxtel et al. (1998) who collected the sEMG signal with pairs of Ag-AgCl electrodes of 2 mm diameter spaced 12 to 36 mm apart. The compatibility of the results infers that the preferred corner frequency transcends electrode geometry. But it differs from others in the literature, such as the 5 Hz high-pass corner frequency recommended by Merletti (1999), which is currently endorsed by the International Society of Electrophysiology and Kinesiology (ISEK) and the 10 Hz high-pass corner frequency required by the Journal of Electromyography and Kinesiology. However, it is consistent with the original recommendation of ISEK (Winter et al., 1980).

Conflict of interest statement

Acknowledgements

Appendix A. Supplementary Material

Supplementary data associated with this article can be found in the online version at doi:10.1016/j.jbiomech.2010.01.027.

References

Adam, A., De Luca, C.J., 2005. Firing rates of motor units in human vastus lateralis muscle during fatiguing isometric contractions. Journal of Applied Physiology 99, 268–280.

Basmajian, J.V., De Luca, C.J., 1985. Muscles Alive 5th edition Williams and Wilkins, Baltimore.

Beck, T.W., Housh, T.J., Cramer, J.T., Malek, M.H., Mielke, M., Hendrix, R., Weir, J.P., 2008. Electrode shift and normalization reduce the innervation zone's influence on EMG. Medicine and Science in Sports and Exercise 40, 1314–1322.

De Luca, C.J., 1997. The use of surface electromyography in biomechanics. Journal of Applied Biomechanics 13, 135–163.

Gamet, D., Duchene, J., Garapon-Bar, C., Goubel, F., 1993. Surface electromyogram power spectrum in human quadriceps muscle during incremental exercise. Journal of Applied Physiology 74 (6), 2704–2710.

Huigen, E., Peper, A., Grimbergen, C.A., 2002. Investigation into the origin of the noise of surface electrodes. Medical and Biological Engineering and Computing 40, 332–338.

LeFever R.S. and De Luca C.J., 1976. The contribution of individual motor units to the EMG power spectrum. In: Proceedings of 29th Annual Conference on Engineering in Medicine and Biology, Boston, p. 56.

Lindstrom, L.R., Magnusson, R., Petersen, I., 1970. Muscular fatigue and action potential conduction velocity changes studied with frequency analysis of EMG signals. Electromyography 4, 3341–3353.

Merletti, R., 1999. Standards for reporting EMG data. Journal of Electromyography and Kinesiology 9, 1.

Pullman, S.L., Goodin, D.S., Marquinez, A.I., Tabbal, S., Rubin, M., 2000. Clinical utility of surface EMG: report of the therapeutics and technology assessment subcommittee of the American Academy of Neurology. Neurology 55 (2), 171–177.

Roy, S.H., DeLuca, C.J., Casavant, D.A., 1989. Lumbar muscle fatigue and chronic lower back pain. Spine 14, 992–1001.

Roy, S.H., De Luca, G., Cheng, S., Johansson, A., Gilmore, L.D., De Luca, C.J., 2007. Electro-mechanical stability of surface EMG sensors. Medical and Biological Engineering and Computing 45, 447–457.

Saitou, K., Masuda, T., Michipkami, D., Kojima, R., Okada, M., 2000. Innervation zones of the upper and lower limb muscles estimated by using multi-channel surface EMG. Journal of Human Ergology 29, 35–52.

Stegeman D.F. and Hermens H.J., 1998. Standards for surface electromyography: the European project (SENIAM). In: Hermens H.J., Rau G., Disselhorst-Klug C., Freriks B. (Eds.), Surface Electromyography Application Areas and Parameters. Proceedings of the Third General SENIAM Workshop on surface electromyography, Aachen, Germany, pp. 108–112.

van Boxtel, A., Boelhouwer, A.J.W., Bos, A.R., 1998. Optimal EMG signal bandwidth and interelectrode distance for the recording of acoustic, electrocutaneous, and photic blink reflexes. Psychophysiology 35, 690–697.

van Boxtel, A., 2001. Optimal signal bandwidth for the recording of surface EMG activity of facial, jaw, oral, and neck muscles. Psychophysiology 38, 23–34.

Winter D.A., Rau G., Kadefors R., Broman H., and De Luca C.J., 1980. Units, terms and standards in the reporting of EMG research. A Report of the ad hoc Committee of the International Society of Electrophysiological Kinesiology.